Scientific Research Publishing

Advances in Bioscience and Biotechnology, 2022, 13, 188-206
https://www.scirp.org/journal/abb
ISSN Online: 2156-8502
ISSN Print: 2156-8456

Anti-Angiogenic and Anti-Metastatic Effects of Biogenic Silver Nanoparticles Synthesized Using *Azadirachta indica*

Shedrack Reuben Kitimu[1,2*], Peter Kirira[3], Ahmed A. Abdille[1], Judith Sokei[1], Dominic Ochwang'i[4], Peter Mwitari[5], Andrew Makanya[4], Naomi Maina[1,6]

[1]Department of Molecular Biology and Biotechnology, Pan-African University, Nairobi, Kenya
[2]Department of Veterinary Physiology, Biochemistry and Pharmacology, Sokoine University of Agriculture, Morogoro, Tanzania
[3]Department of Physical Sciences, Mount Kenya University, Kiambu, Kenya
[4]Department of Veterinary, Anatomy and Physiology, University of Nairobi, Nairobi, Kenya
[5]Centre for Traditional Medicine and Drug Research, Kenya Medical Research Institute, Nairobi, Kenya
[6]Department of Biochemistry, Jomo Kenyatta University of Agriculture and Technology, Nairobi, Kenya

Email: *srkitimu25@sua.ac.tz

How to cite this paper: Kitimu, S.R., Kirira, P., Abdille, A.A., Sokei, J., Och-wang'i, D., Mwitari, P., Makanya, A. and Maina, N. (2022) Anti-Angiogenic and Anti-Metastatic Effects of Biogenic Silver Nanoparticles Synthesized Using *Azadirachta indica*. *Advances in Bioscience and Biotechnology*, **13**, 188-206.
https://doi.org/10.4236/abb.2022.134010

Received: March 1, 2022
Accepted: April 12, 2022
Published: April 15, 2022

Abstract

Background: Nanotechnology symbolizes a broad discipline with enormous potential in cancer treatment bridging one of the bottlenecks of traditional approaches in cancer therapy which is an inability to deliver adequate quantities of anti-cancer drugs to the tumor area. Studies on nanoparticles indicate their importance in cancer angiogenesis and metastasis. **Aim:** The present study assessed anti-angiogenesis and anti-metastatic effects of biogenic silver nanoparticles (AgNPs) synthesized from neem plant (*Azadirachta indica*). **Methods:** Chicken chorioallantoic membrane (CAM) and two-dimensional (2D) wound healing assays were used to study anti-angiogenic and anti-metastatic effects of the AgNPs respectively. Twenty-four fertilized eggs were divided into four groups: two biogenic AgNPs treatments at 100 µg/ml and 200 µg/ml; negative control (1% DMSO) and positive control (cyclophosphamide). On day 8 of incubation, filter discs impregnated with different concentration levels of the treatments were placed on the CAM. On day 12 of incubation, the CAMs were imaged using a stereomicroscope, scaled using ImageJ, and different morphometric and spatial parameters computed using AngioTool software. Vessel area, vessel percent area, total number of junctions, total vessel length, average vessel length, mean lacunarity, and junction density were measured. The crown-rump length (CRL) and fetal weight were also recorded on day 16 of incubation. In order to determine relative gene expression profiles of iNOS and VEGF, total RNA was extracted from the CAM, and qRT-PCR was performed with β-Actin as a reference gene. For the

2D wound healing assay, DU145 human prostate cells were grown in Dulbecco's Modified Eagle's Medium supplemented with 10% Fetal Bovine Serum. **Results:** Biogenic AgNPs demonstrated anti-angiogenic effects in a dose-dependent manner in the parameters generated from the CAM images. Also, qRT-PCR revealed down-regulation of iNOS and VEGF genes. The 2-dimensional wound healing assay showed inhibition of migration and motility of the DU145 cells for the 72-hours of assessment. **Conclusion:** The present study postulates that the biogenic AgNPs can prevent angiogenesis by inactivation of VEGF-NO and VEGF/VEGF-R pathways while inhibiting cell migration and metastasis.

Keywords

Biogenic AgNPs, Cancer, Angiogenesis, Metastasis, CAM

1. Introduction

Cancer emerges as one of the prime health problems in Africa that require immediate and appropriate measures in order to combat its increased incidence and mortality rates [1]. By the year 2030, about a 70% increase in new cancer cases will be attributed to population increase and aging [1]. Current cancer treatment methods include surgery, chemotherapy, radiotherapy, gene therapy, stem cell therapy, and hormone-based therapy, most of which are already experiencing treatment failure. The greatest cause of failure of cancer therapy is attributed to the spread of cancer cells from a primary tumor to other tissue to seed secondary tumors, referred to as metastasis [2]. Secondary to that, the available drugs are hampered by low delivery and high toxicity issues rendering the entire treatment regime ineffective.

There is an increase in interest and use of plant-based therapies since plant-derived products have shown promise in treating different cancer types such as colorectal, breast, prostate, stomach, esophageal and liver cancer among others [3]. Many plant species are already being used to treat or prevent the development of cancer [3] [4]. Neem plant (*Azadirachta indica*) has been reported to possess a number of activities such as antimicrobial, antidiabetic, antifertility, cardioprotective and anti-cancer properties among others [5]. Phytochemicals present in the neem plant have been also demonstrated to have anticancer activities against cervical, breast, prostate and colorectal cancer both *in vitro* and *in vivo* [5] [6]. However, the use of plant-derived products in the treatment of cancer faces a number of bottlenecks such as limited bioavailability of active phytochemicals to the target cells and toxicity [7]. This prompts the need for targeted therapy that improves the drug delivery system and minimizes side effects through nanotechnology [8]. The latter entails the use of biocompatible and biodegradable systems that can escalate the bioavailability and the concentration of conventional drugs at the desired site, as well as improve the release profile in

the tumor area [9].

Nanotechnology has been employed to target different mechanisms tied to cancer growth and progression such as metastasis and angiogenesis [10] [11]. The latter is a physiological process arising from preexisting vessels and critical in embryogenesis and maintaining homeostasis, including repair and regeneration of damaged tissues among others [12]. Though the process can be deregulated in some disease conditions, it can be switched on during malignancies due to an increase in angiogenic stimulators such as tumor angiogenesis factors (TAFs). This is secreted by tumor cells in response to the need for nutrients and oxygen promoting cancer growth and progression [12]. Therefore, targeting angiogenesis is viewed as an important therapeutic strategy in the medical setting and particularly for cancer therapy. Several molecular mechanisms and pathways have been implicated and considered potential targets including VEGF/VEGFR, PDGFB/PDGFR-b, iNOS pathway, and the angiopoietins [13] [14]. Of three nitric oxide synthase (NOS) synthesized by mammalian cells, iNOS expressed after cytokine exposure has shown to generate more NO than other constitutive members nNOS and eNOS and modulate important cancer related processes such as angiogenesis and metastasis [15]. Upregulation of Nitric oxide synthase (NOS) promotes a number of pro-angiogenic factors such as VEGF, fibroblast growth factor (FGF2), and Ang2 where inhibition of eNOS or iNOS was found to arrest angiogenesis in rat models [16]. Angiogenesis can help in metastasis; a process where tumor cells invade the blood vessels, circulate and re-invade out at the distant sites and proliferate. This is because the vascular network developed by cancer cells not only provides nutrients for the tumor but also serves as an escape route for the tumor cells to enter circulation [17].

Given the limitations of the available cancer drugs, nanomaterials reported in literature indicate the potential for cancer metastasis and angiogenesis [18]. A good number of nanoparticles have been demonstrated to possess good antiangiogenic and anti-metastatic properties both *in vitro* and *in vivo* [11] [12] [13]. However, apart from its antimicrobial properties which are well known, angiogenesis and metastasis modulation of silver nanoparticles (AgNPs) and the mechanisms involved are yet to be fully understood. Nevertheless, it was reported that silver nanoparticles biosynthesized in *Bacillus licheniformis* biomass inhibited the proliferation and migration of bovine retinal endothelial cells supplemented with exogenous VEGF, as well as micro-vessel formation in the mice model which was attributed to the inactivation of the PI3K/Akt signaling pathway [19].

Azadirachta indica extracts have been also encapsulated in various metallic nanoparticles (NPs) such as silver and gold [20]. Silver nanoparticle (AgNPs) is one of the most studied and utilized nanoparticles in drug formulation due to its potent broad spectrum of activities, extremely large surface area, strong permeability and little drug resistance [6] [21]. Recently, we formulated and characterized silver nanoparticles using bark methanolic extracts of *Azadirachta indica* (neem) of average size 58 nm that showed good activity in anti-proliferation of

DU145 human prostate cancer and low cytotoxicity to normal cell Vero E7 [22]. The NPs also had a superior selectivity index compared to that of the control drug (doxorubicin) and therefore shown to be promising as a suitable anticancer agent. The present study further elucidated the potentials of the NPs in inhibiting angiogenesis and metastasis using chicken chorioallantoic membrane (CAM) assay and wound healing assay respectively. Also, this study explored the activity of the NPs in the expression of angiogenesis related genes (iNOS and VEGF) to uncover possible molecular mechanisms involved in angiogenesis.

2. Materials and Methods

2.1. Materials

Silver nanoparticles (AgNPs) previously biosynthesized from methanolic extracts of neem plant (*Azadirachta indica*) stem bark and characterized using FTIR, UV Vis Spectroscopy, zeta sizer and zeta potential; and reported in the previous research of our group by Kitimu *et al.*, [22] were used in this study. Also, freshly fertilized eggs of local improved chicken (*Gallus domesticus*) developed by the Kenya Agricultural and Livestock Research Organization (KALRO) were purchased from Neochicks Poultry Limited, Kenya.

2.2. Chicken Chorioallantoic Membrane Assay

Following a protocol used by Lokman *et al.* [23], with modifications, the fertilized eggs were cleaned with a white clean towel soaked in distilled water and air dried before they were incubated in an Eteyo incubator (model: JN5-60) at 37˚C with 60% humidity. The eggs were manually rotated at least twice a day during incubation. On day 3 of incubation, a small window was made on the shell aseptically using a scalpel blade and forceps. Before that, 2 - 3 ml of albumin was aspirated from the sharp end of the egg at a 45˚ angle using a 5 ml hypodermic syringe in order to drop the developing chicken chorioallantoic membrane and also simplify the window opening. The window was resealed with adhesive tape and eggs were returned to the incubator until day 8 of chick embryo development. On day 8, the windows were opened and sterile filter discs previously treated with different concentrations of biogenic AgNPs added to the CAM. Negative control received vehicle 1% DMSO, positive control received 100 µg/ml cyclophosphamide (Sigma Aldrich) and two treatments of the biogenic AgNPs at two different concentrations of 100 µg/ml and 200 µg/ml. Eggs were resealed and returned to the incubator on day 12 (n = 6 chicken embryos per treatment). On day 12, the seal was removed aseptically and all the cases were photographed using a Nicon D5100 (Nicon, Corporation) camera fitted at the eyepiece of an Olympus SZ61 stereomicroscope (Olympus Corporation, Japan). The images were analyzed using both ImageJ and Angiotool software. Scores were computed as a result of the correlation between pixels in the image and an alternative unit length in the sample in which AngioTool uses millimeters as a unit of length. The obtained angiogenic parameters included vessel area, vessel percent area,

the total number of junctions, total vessel length, average vessel length, mean lacunarity and junction density.

Also, following protocol by Baharara *et al.*, [24], and later by Bokariya *et al.*, [25], the eggs were again resealed and put back in the incubator until day 16 when morphometric data (crown-rump length and fetal weight) were recorded. In the course, eggs were occasionally checked for mortality through candling and dead embryos were removed. While the fetal weight was measured using a digital weighing balance, the crown-rump length was measured by passing a thread from the root of the beak along the back to the tip of the coccyx and later measuring the corresponding length of the thread using a ruler in centimeters (cm).

2.3. Two-Dimensional Wound Healing Assay

2.3.1. Cells

DU 145 human prostate cancer cells obtained from ATCC (Manassas, VA, USA) were used. As in Kitimu *et al.*, [22], the cells were grown in MEM medium supplemented with 10% Fetal Bovine Serum (FBS), 1% L-Glutamine and 1% antibiotic (Penicillin/Streptomycin) in a T75 culture flask and incubated at 37˚C and 5% CO_2 to attain confluence of 80%. The cells were sub-cultured in 12 wells plates for the wound healing assay.

2.3.2. Wound Infliction and Measurement

As previously described by Abdille *et al.*, [26], DU-145 cells were counted and plated in 12-well plates with a cell density of 5×10^4 cells/well. Cell growth was monitored until the cells attained 95% confluence where a wound was inflicted on the cell monolayer using a sterile 200 µl tip. The media with its associated debris were removed and washed with PBS before the addition of 1.5 ml of media containing either biogenic AgNPs (15 µg/ml and 30 µg/ml) and positive control (cyclophosphamide at 100 µg/ml) to the wells. Negative control received the media together with 1% DMSO solvent. The concentrations of the biogenic AgNPs used *i.e.* 15 µg/ml and 30 µg/ml were $2IC_{50}$ and $4IC_{50}$ respectively of the pre-determined IC_{50} and previously reported [22]. After treatment, cells were monitored for their progress and photographs were captured using a Nicon D5100 (Nicon, Corporation) camera fitted at the eyepiece of the inverted microscope at time intervals 0, 24, 48 and 72 hours. Wound recovery (depicted by the size of the wound) was assessed during the time-points of the treatments.

2.4. Relative Gene Expression

2.4.1. RNA Extraction

Using a different set of experiments employing chicken chorioallantoic membrane (CAM) assay as described earlier, the CAMs were treated on day 8 with either biogenic AgNPs (100 µg/ml and 200 µg/ml) or positive control (cyclophosphamide) while negative control received 1% DMSO vehicle. After 24 hours (day 9), the CAMs were collected and snap-frozen in liquid nitrogen and transferred to a −80˚C freezer. Whole CAM was ground in liquid nitrogen and a por-

tion of about 50 mg was used for RNA extraction using *Quick*-RNA Miniprep Kit (Zymo Research) as described by the manufacturer. The total RNA quantity and purity were determined by spectrophotometric analysis. The quality of the RNA was confirmed by 1% agarose electrophoresis.

2.4.2. cDNA synthesis

cDNA synthesis was done using FIREScript RT cDNA Synthesis kit (Solis Bio-Dyne, Estonia) following the manufacturer's instructions and previously used by Nirmali *et al.* [27]. Briefly, a 20 µL reaction mix was prepared by mixing 10 µl of (100 µg/ml) of RNA, 1 µl Oligo (dT) primer (100 µM), 2 µl of 10x RT Reaction Buffer with DTT, 0.5 µl dNTP Mix (20 mM), 1 µl FIREScript RT, 0.5 µl RNase Inhibitor (40 U/µl) and 5 µl of nuclease-free water. The mixture was incubated at 55˚C for 30 minutes and the enzyme was inactivated at 85˚C for 5 minutes.

2.4.3. Primer Design

Primers used were designed using the National Center for Biotechnology Information's (NCBI) Primer Blast tool (https://www.ncbi.nlm.nih.gov/tools/primer-blast/) while reference sequences of the genes were retrieved from GenBank in FASTA format. Sequence manipulation suite (https://www.bioinformatics.org/sms2/pcr_primer_stats.html) was used to test each pair of primers obtained considering GC contents, primer melting temperature (Tm) and hairpin formation. Product size of 80 to 250 bp was targeted. All primers with a pass record were checked for Tm using oligoCalc (http://biotools.nubic.northwestern.edu/OligoCalc.html). Prior to qRTPCR, the primers were optimized using conventional PCR and upon gel electrophoresis, the primers that presented the expected sizes of the products were used for downstream application (Table 1).

2.4.4. qRT-PCR

Relative gene expression was studied using qRT-PCR real time thermal cycler qTOWER3 84 GmbH (Analytik Jena). The qRT-PCR reaction was performed using 2X qRT-PCR Master Mix (Beijing Solarbio Science & Technology Co.,

Table 1. Primers used for qRT-PCR.

Gene name	Sequence 5'-3'		Annealing temperature	PCR product size (bp)	GeneBank number
β-Actin	F	CTGAGAGTAGCCCCTGAGGA	61	185	EU309690.1
	R	CACAGCCTGGATGGCTACAT			
iNOS	F	TTGGAAACCAAAGTGTGT	61	95	JQ280464.1
	R	CCCTGGCCATGCGTACAT			
VEGF	F	CGGTACAAACCACCCAGCTT	61	139	AY168004.1
	R	TGTCCAGGCGAGAAATCAGG			

Abbreviations: F: forward; R: reverse; iNOS: inducible nitric oxide synthase; VEGF: vascular endothelial growth factor.

Ltd) following the manufacturer's instructions. A 25 µl reaction contained 12.5 µl of the 2X master mix, 1 µl each of the forward and reverse primers (10 pmol/µl), 1 µl of cDNA and 9.5 µl of nuclease-free water. All reactions were carried out in triplicate. The qRTPCR was done using the program; initial denaturation: 95˚C for 10 minutes; denaturation at 95˚C for 20 seconds, annealing at 61˚C for 45 seconds, final elongation after 35 cycles at 72˚C for 5 minutes. Also, the melting curve was generated at the temperature range of 60˚C to 95˚C. **Table 1** shows the list of primers used for real-time PCR analysis. *β*-actin was used as an internal control for inducible Nitric Oxide synthase (iNOS) and vascular endothelial growth factor (VEGF) expression.

2.5. Data Analysis

ImageJ software was used for image scaling while AngioTool software (AngioTool v 0.6a (02.18.14)) was used to compute several morphological and spatial parameters. Statistical analyses of the experimental data were performed using GraphPad Prism 8.4.3 software (Graph-Pad Software, San Diego, CA). The data were recorded as numbers and expressed as means ± SEM. Further statistical investigations were done using a t-test (Mann-Whitney). On the other hand, the relative expression levels of the target genes were calculated using the delta-delta Ct ($2^{-\Delta\Delta Ct}$) method and results were subjected to One-way ANOVA followed by Tukey test post hock analysis for multiple comparisons. The house-keeping gene *β*-Actin was used as a reference gene to normalize the expression of the target genes. In each case, *p*-values less than 0.05 were considered significant.

2.6. Ethical Approval

Approval for experimentations was granted by the University of Nairobi Animal Ethics Committee at the department of veterinary physiology and anatomy and issued in a letter with reference number: FVM BAUEC/2021/308.

3. Results

3.1. Chicken Chorioallantoic Membrane Assay

We compared CAM images generated from two treatments of biogenic AgNPs (200 µg/ml and 100 µg/ml) including a negative (vehicle 1% DMSO) and positive (cyclophosphamide) controls. Images were assigned scales using ImageJ and analyzed with AngioTool v 0.6a (02.18.14) software. The original images and those resulting after processing (skeletonized) are shown in **Figure 1**. The measurements of the vessel area, vessel percent area, total number of junctions, total vessel length and average vessel length are shown (**Figure 2**) where antiangiogenic effects of the biogenic AgNPs are in a dose-dependent manner. There was a significant difference ($p < 0.05$) between the treatments and negative control for the total number of junctions, total vessel length and average vessel length. Conversely, save for average length, there was a significant difference ($p < 0.05$) in all parameters between positive control and other treatments.

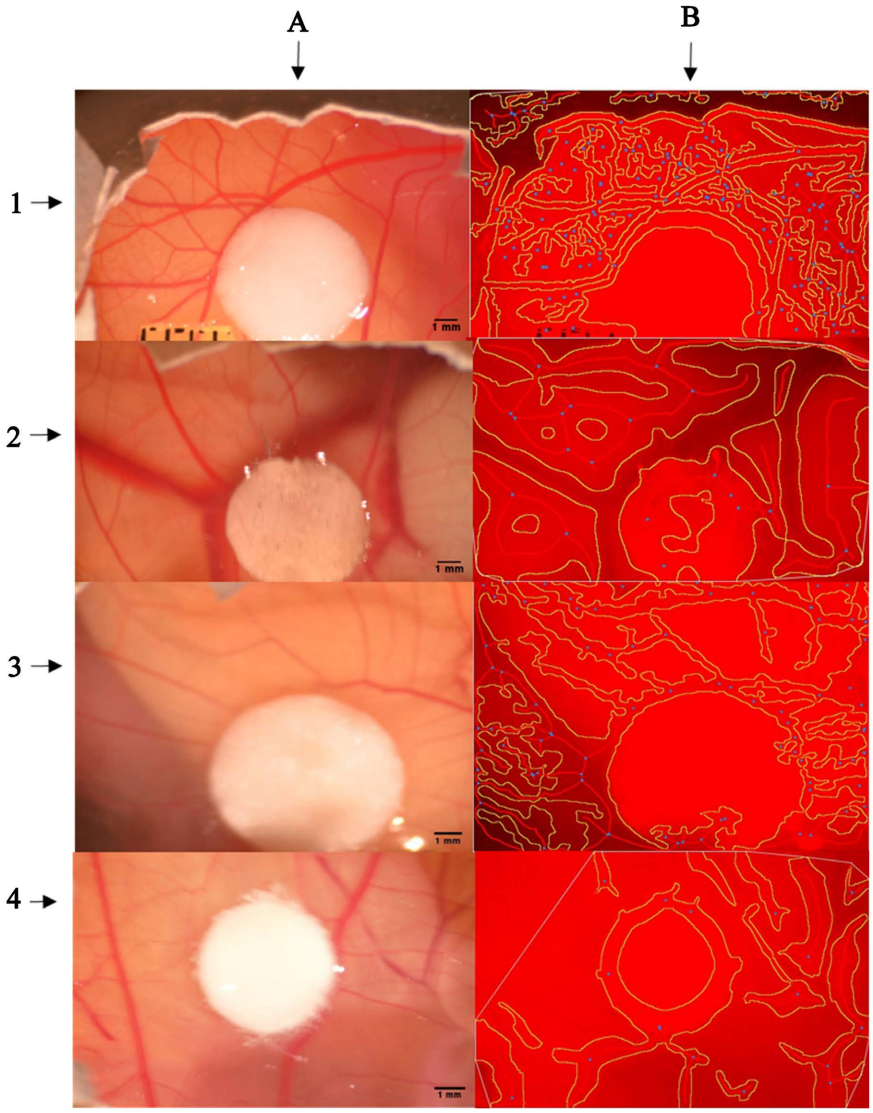

Figure 1. Analysis of angiogenesis in biogenic AgNPs treated CAM. (1): Representative images of CAM from negative control (1% DMSO); (2): Treated group with 100 μg/ml biogenic AgNPs; (3): Treated group with 200 μg/ml biogenic AgNPs; (4): Representative images of CAM from positive control (cyclophosphamide); (A): Original CAM images with scales (left); (B): The resulting images after processing (right). The vessel outlines are shown in yellow, the skeletons in red and the branching points in blue as computed by AngioTool v 0.6a (02.18.14) software.

Further assessment was done on the extent to which the treatments inhibited angiogenesis by fractal analysis using junction density and lacunarity measures. Angiogenesis was inhibited in a dose-dependent manner and there was a significant difference ($p < 0.05$) between the treatments and controls (Figure 3). In this case, the greater the vascular density, the more angiogenesis is believed to have occurred. On the other hand, lacunarity characterizes the distribution of gaps in the fractal in which a fractal with high lacunarity has large gaps. In this case, positive control had lower vascular compared to other treatments indicating the antiangiogenic activities of the control. The higher dose of biogenic AgNPs (200

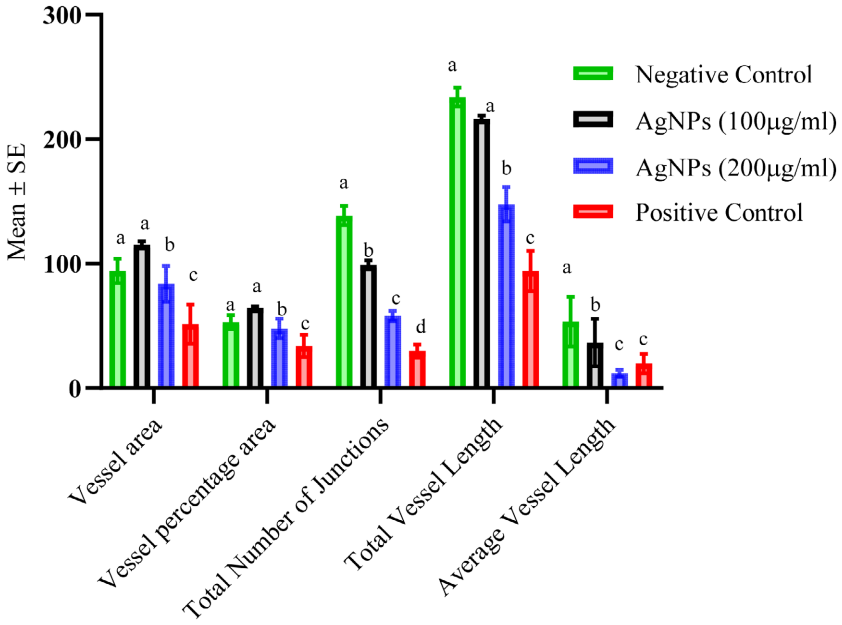

Figure 2. Graphical representations of the analysis performed on different groups (N = 6). Differences in letters indicate significant difference ($p < 0.05$) between groups Statistical analysis.

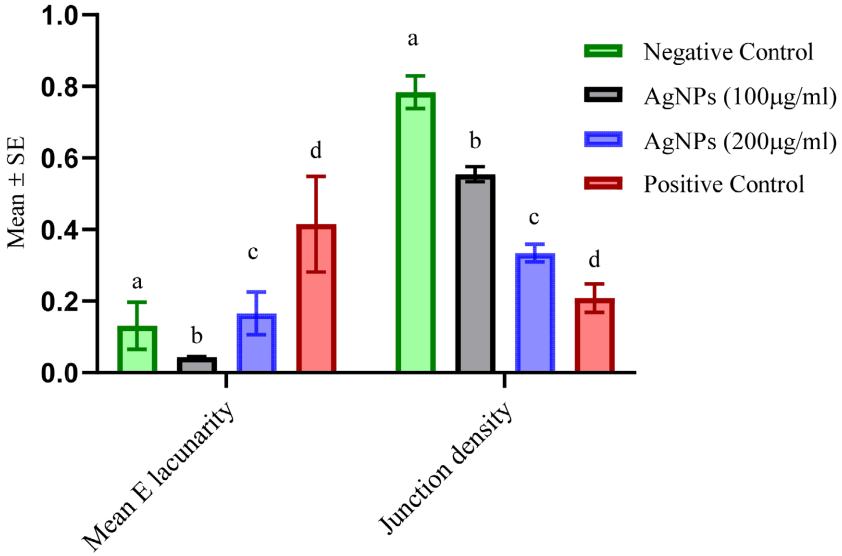

Figure 3. Fractal analysis indicates junction density and mean lacunarity for the different treatments. Antiangiogenic activities were dose-dependent with the positive control exhibiting more activities.

µg/ml) had lower vascular density compared to that of 100 µg/ml. The lacunarity values for the positive control were higher compared to the rest of the treatments in which also the higher dose of biogenic AgNPs (200 µg/ml) showed higher lacunarity compared to the lower dose (100 µg/ml).

Effects of the treatments on the morphometric parameters were also analyzed in which body weight of the fetuses and crown-rump length were measured and graphical presentation is shown in Figure 4 & Figure 5. The fetal body weights

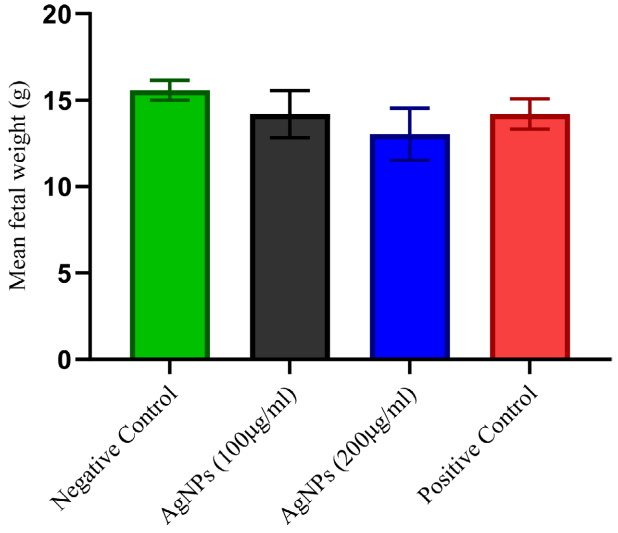

Figure 4. Effects of biogenic AgNPs on fetal body weight.

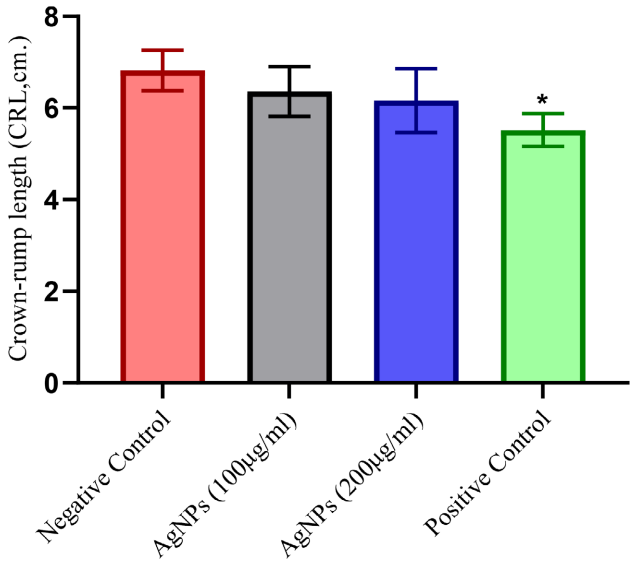

Figure 5. Effects of biogenic AgNPs on crown-rump length (CRL). The CRL were reduced in a dose dependent manner where the positive control showed a significant difference ($p < 0.05$) from the negative control indicated by the asterisk.

in brackets for different treatments were; negative control (15.58 ± 0.57 cm), 100 µg/ml (14.2 ± 1.4 cm), 200 µg/ml (13.04 ± 1.51 cm) and positive control (14.2 ± 0.9 cm). There was no significant difference between treatment groups and controls ($p > 0.05$). In addition, crown-rump length (CRL) did not show a significant difference between the treatments from the negative control. However, the positive control reduced the CRL significantly from the negative control.

3.2. Wound Healing Assay

The anti-metastatic effects of biogenic AgNPs were studied alongside positive control (cyclophosphamide) using cell migration assay (wound healing) and the results are indicated in **Figure 6**. Results show that biogenic AgNPs was able to

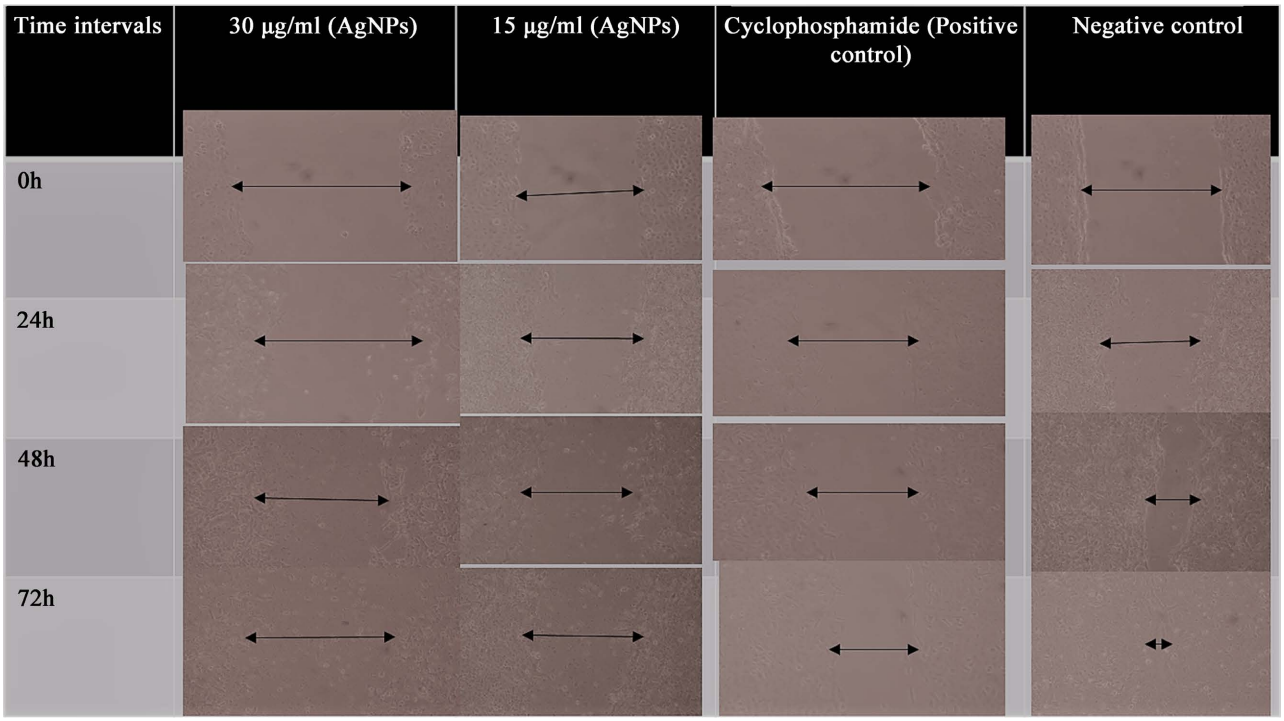

Figure 6. Wound healing assay. Effect of biogenic AgNPs on the migration of the cells from time 0 to 72 hours. Arrows indicate the size of the wound during the entire duration (each image was taken at 10× magnification under inverted microscope).

inhibit cells from migrating to the opening and thus delayed recovery of the wound. It is evident from the images that in the negative control, wound closure was able to occur after 72 hours. The stronger effects were observed when the highest concentration of 30 µg/ml biogenic AgNPs was used. In this case, the AgNPs induced death of some cells as they could be seen floating on the media.

3.3. Relative Gene Expression

The effect of biogenic AgNPs on the expression profiles of iNOS and VEGF was explored. Both biogenic AgNPs and positive (cyclophosphamide) significantly down regulated the expression of all the targets (**Figure 7** & **Figure 8**). Different letters on each bar indicate a significant differences ($p < 0.05$) resulting from One way AVOVA followed by Tukey's multiple comparison post hoc analysis carried out in Graph Pad Prism software (v8.4.3). Asterisk (*) indicates significant difference ($p < 0.05$) from negative control following post hoc analysis. Higher fold changes were observed in the highest dose of biogenic AgNPs (200 µg/ml). The increase in the NPs concentrations therefore increased the activity of the drug in the down-regulation of the target genes (**Table 2**).

4. Discussion

Cancer remains the global health burden owing to the lack of effective therapy. The ineffectiveness of the available anti-cancer drugs is attributed to the spread of cancer cells from a primary tumor to other tissues and also hampered by low delivery and high toxicity. As a result, there is an increase in interest and use of

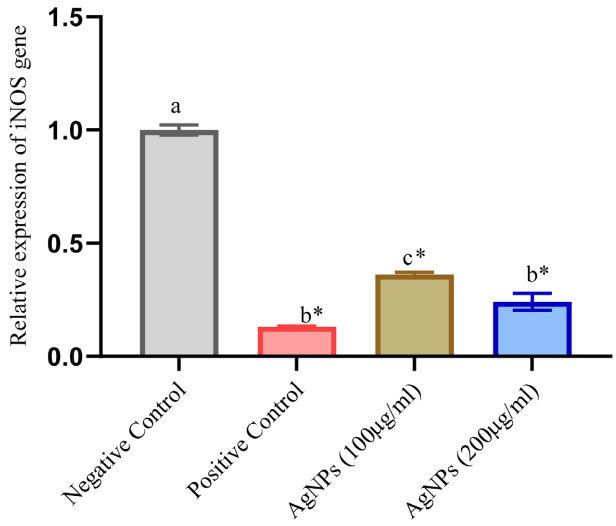

Figure 7. iNOS expression on CAM treated with biogenic AgNPs. AgNPs inhibited angiogenic specific gene expression on chicken chorioallantoic membrane. Different letters on each bar indicate significant differences ($p < 0.05$) resulting from One way AVOVA. Asterisk (*) indicates a significant difference ($p < 0.05$) from negative control following post hoc analysis.

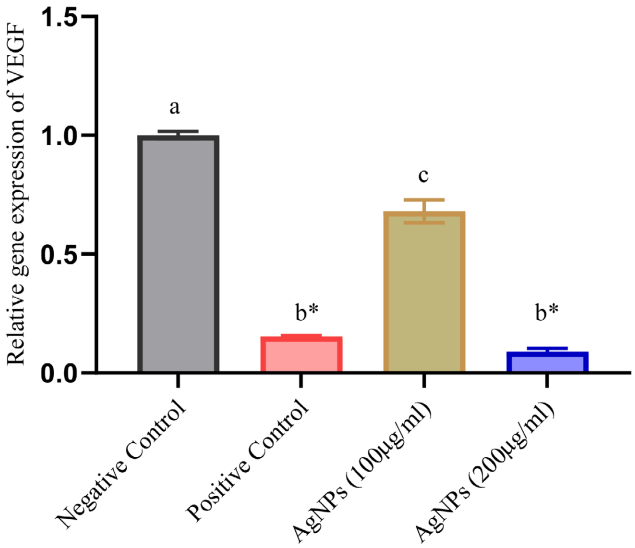

Figure 8. VEGF expression on CAM treated with biogenic AgNPs. AgNPs inhibits angiogenic specific gene expression on chicken chorioallantoic membrane. Different letters on each bar indicate significant differences ($p < 0.05$) resulting from One way AVOVA. Asterisk (*) indicates a significant difference ($p < 0.05$) from negative control following post hoc analysis.

Table 2. Relative gene expression of target genes (iNOS and VEGF) following treatments with biogenic AgNPs.

Groups	Negative control	Positive control	AgNPs (100 µg/ml)	AgNPs (200 µg/ml)
2^-ddct (iNOS)	1.00 ± 0.016	0.153 ± 0.004	0.68 ± 0.048	0.089 ± 0.014
2^-ddct (VEGF)	1 ± 0.02	0.13 ± 0.004	0.36 ± 0.01	0.24 ± 0.04
Fold change (iNOS)	1	6.54	1.47	11.25
Fold change (VEGF)	1	7.61	2.76	4.14

plant-based therapies since plant-derived products have shown promise in treating different cancer types. Neem plant (*Azadirachta indica*) among other plants has been reported to possess anti-cancer activities [6] [22] [28]. However, the use of plant-derived products in the treatment of cancer faces a number of bottlenecks such as limited bioavailability of active phytochemicals to the target cells and toxicity [7]. It has therefore prompted targeted therapy that could improve the drug delivery systems and minimize side effects through nanotechnology [8].

The current study investigated anti-angiogenic and anti-metastatic activities of biogenic AgNPs synthesized from methanolic extracts of *Azadirachta indica* stem bark using chicken chorioallantoic membrane (CAM) assay and wound healing assay respectively. Further, using the CAM assay, we explored the effects of the NPs on gene expression implicated with angiogenesis (iNOS and VEGF) using cyclophosphamide as a positive control. Results elucidated that biogenic AgNPs have an anti-angiogenic effect on the CAM and anti-metastatic activity against DU-145 human prostate cancer cells.

Angiogenesis is a physiological process involving the formation of new blood vessels from the pre-existing vascular bed. It also plays as one of the hallmarks of cancer, implicated in tumor growth, invasion and metastasis [12]. In view of this and since tumor blood vessels are genetically unstable and different from normal vessels, they are potential targets in therapy for all types of cancer. CAM has been extensively used in studying angiogenesis, tumor cell invasion and metastasis with advantages over other methods due to its highly vascularized nature promoting the efficiency of tumor cell grafting, high reproducibility; simplicity and cost-effectiveness [23] [29]. In this study, anti-angiogenesis was evident following a significant reduction in spatial parameters including vessel area, vessel percent area, total number of junctions, total vessel length, average vessel length and junction density in a dose-dependent manner. Also, together with the positive control (cyclophosphamide), the angiogenesis related genes hereby assessed were significantly down-regulated by the biogenic AgNPs suggesting its potential anti-cancer activities targeting the pathways implicated with these genes during angiogenesis. For lacunarity which characterizes the distribution of gaps in the fractal, there was a significant increase in high concentration (200 μg/ml) NPs treated groups and positive control compared to the negative control that suggests antiangiogenic properties of the biogenic AgNPs at high dose.

Morphometric parameters were analyzed in this study in order to uncover the effects of the treatments on embryo development. Results showed a decrease in the body weight of the embryos in a dose-dependent manner. However, no significant difference was observed in all groups. Also, crown-rump length (CRL) did not show a significant difference between the treatments from the negative control except for the positive control which reduced the CRL significantly. Therefore, biogenic AgNPs do not affect embryo development and shows no toxicity to the embryo. Some studies reported on the toxicity of NPs that can

lead to a significant generation of reactive oxygen species (ROS) and upregulation of genes involved in cellular stress and toxicity [30] that could possibly lead to a decrease in body weight. Such an observation was reported in broiler chicken treated with a high concentration of gold nanoparticles [31]. Morphometric analysis for the current study was meant to check the possible toxicity the biogenic AgNPs can impose by changing the parameters measured. That was not the case as no evidence of toxicity was recorded and for that reason, the biogenic AgNPs from bark methanolic extracts of *Azadirachta indica* can be considered safe for use as an anti-cancer agent.

Our findings concur with other reports where biogenic AgNPs synthesized using *Saliva officinalis* elucidated antiangiogenic properties on CAM by significantly reducing the average number and length of blood vessels [24]. The results are also in line with that of AgNPs biosynthesized in *Bacillus licheniformis* biomass (with an average size of 500 nm) exhibiting the anti-angiogenic, anti-proliferative and anti-migratory activities of bovine retinal endothelial cells supplemented with exogenous VEGF which was attributed to the inactivation of the PI3K/Akt signaling pathway by the NPs [19]. However, the results conflict with another study where poly (vinyl pyrrolidone)-coated AgNPs (with size 2.3 nm) presents pro-angiogenic properties both *in vitro* and *in vivo* through the generation of reactive oxygen species (ROS) and production of angiogenic factors like VEGF and nitric oxide (NO) [32]. Moreover, the silver nanoparticles up regulated FAK, Akt, ERK1/2, and p38, which were all involved in the VEGFR-mediated signaling pathway. The reported proangiogenic effects could be due to the presence of the surface polymer coating and the smaller size of the NPs compared to other studies reporting on an anti-angiogenic potential of AgNPs [12] including the present study which used NPs of average size of 58 nm.

In this study, angiogenesis-related genes (iNOS and VEGF) were downregulated with fold changes that were apparently dose-dependent. The results are consistent with the reduction in angiogenic markers, iNOS and VEGF-A after treatment with Res-nanoparticles in cancer, stem-like-enriched oral cancer cells niche at a fold change of 2.5 and 5.1 respectively [33]. Research in tumor angiogenesis discovered the main molecular drivers of tumor angiogenesis, the vascular endothelial growth factor (VEGF) family forming the dominant target for antiangiogenic drugs owing to its ubiquitous nature and more importantly upregulated in most human cancers [13]. VEGF elucidates proangiogenic effect through activation of VEGF/VEGF-receptor pathway [34]. Results from the current study demonstrate the role biogenic AgNPs played in downregulating VEGF by probably inactivating the VEGF/VEGF-receptor pathway. AgNPs biosynthesized from Rapeseed pollen were also able to downregulate VEGF and therefore suppress breast cancer carcinogenesis [35]. Also, Gurunathan *et al.* [19], reported potential of AgNPs biosynthesized from *Bacillus licheniformis* biomass to inhibit VEGF-induced proliferation and migration of bovine retinal

endothelial cells as well as micro-vessel formation in a mice model which was attributed to the inactivation of the PI3K/Akt signaling pathway [19].

On the other hand, iNOS expressed after cytokine exposure generates nitric oxide, an important modulator of some important cancer related processes such as angiogenesis and metastasis [15]. It is also known that upregulation of Nitric oxide synthase (NOS) promotes a number of pro-angiogenic factors such as VEGF, fibroblast growth factor (FGF2), and Ang2 where inhibition of iNOS was found to arrest angiogenesis in rat models [16]. Downregulation of iNOS in this study depicts the role that biogenic AgNPs of bark methanolic extracts can play as a potential anti-cancer agent at molecular level by downregulating activities of NOS and therefore reducing the amount of nitric oxide produced and consequently reduction in the amount of proangiogenic factors released by the cells. iNOS has a profound effect on VEGF expression and their interrelation forms a NO-VEGF axis which forms a target for anticancer agents to inhibit tumor angiogenesis, growth and progression [14]. VEGF promotes angiogenesis through the interaction of NO synthesized by iNOS with the NO sensitive guanylyl cyclase leading to the generation of cyclic guanosine monophosphate (cGMP), which conveys the signals down-stream through a VEGF-NO pathway [36]. For instance, activation of VEGF-NO pathway improved ischemia-induced angiogenesis in rat hind limbs [37]. Generally, the antiangiogenic effects observed from the CAM assay and supported by the downregulation of iNOS and VEGF in the present study partially suggest the activity of the biogenic AgNPs through inactivation of both VEGF-NO and VEGF/VEGF-receptor pathways implicated in angiogenesis.

Regarding the anti-metastatic effects of the biogenic AgNPs, a wound healing assay was conducted. Our findings indicated inhibition of cell migration by biogenic AgNPs against DU-145 prostate cancer cells on a 2D wound healing assay compared to the negative control. There was a total closure of the wound in the negative control after 72 hours of incubation while there was no closure of wounds in NPs treated and positive control. Our results are in line with other findings where AgNPs portrayed anti-migratory effects of AgNPs biosynthesized from *Annona muricata* fruit extracts against HeLa cells [38]. Metastasis contributes to poor prognosis and survival in cancer as cells spread from their primary tumors to distant places [39]. Novel therapeutic agents are therefore important to prevent metastatic from occurring. Our results indicate that Biogenic AgNPs has anti-metastatic effects against DU-145 and be considered a potential anti-cancer drug. These results sync with the anti-angiogenic activities observed above since there is a correlation between angiogenesis and wound healing. For that reason, most of the pro-angiogenic nanofibers have been deployed to accelerate tissue repair and regeneration, especially to stimulate wound healing [40]. When cells fail to recover from the wound inflicted is indicative is the result of inhibition of cell-cell communication hence interfering with of their metastatic potential [39]. When the highest dose was used (30 μg/ml), there was a partial

increase in the size of the wound observed with some floating cells probably due to the cytotoxic effect. We therefore suggest that biogenic AgNPs synthesized using methanolic extracts of *Azadirachta indica* stem bark can be considered as an anti-cancer agent candidate following its good anti-metastatic properties.

5. Conclusion

Biogenic AgNPs from bark methanolic extracts of *Azadirachta indica* elucidated good anti-angiogenic and anti-metastatic activities using chicken chorioallantoic membrane and wound healing assay respectively. Further analysis of gene expression revealed the potential of the NPs to down-regulate angiogenesis related genes (iNOS and VEGF). The gene expression analysis suggested the possible mechanisms through which the NPs use to inhibit angiogenesis which is the inactivation of VEGF-NO and VEGF/VEGF-R pathways. From the results presented in the current work and given the limitations of the available cancer drugs, we advocate further studies on the product including its efficacy and safety assessment *in vivo* in order to generate robust information that could propel its development to clinical trials as one of the novel anti-cancer agents resulting from nanotechnology.

Funding

This study was financially supported by the African Union under the Pan African University Institute for Basic Sciences Technology and Innovation (PAUSTI).

Acknowledgements

Authors extend thanks to the Pan African University for supporting this study. Many thanks are also extended to Ms. Mercy Jepkorir and Mr. Nicholas Adipo of Kenya Medical Research Institute (KEMRI), Centre for Traditional Medicine and Drug Development, also Ms. Milkah Wanjohi of University of Nairobi, Department of Veterinary Physiology and Anatomy for their generous technical supports.

Conflicts of Interest

The authors declare no conflicts of interest regarding the publication of this paper.

References

[1] Jemal, A., *et al.* (2012) Cancer Burden in Africa and Opportunities for Prevention. *Cancer*, **118**, 4372-4384. https://doi.org/10.1002/cncr.27410

[2] Martin, T.A., Ye, L., Sanders, A.J., Lane, J. and Jiang, W.G. (2013) Madame Curie Bioscience Database. Landes Bioscience, Austin.

[3] Roy, A. and Bharadvaja, N. (2017) Medicinal Plants in the Management of Cancer: A Review. *International Journal of Complementary & Alternative Medicine*, **9**, Ar-

ticle No. 291. https://doi.org/10.15406/ijcam.2017.09.00291

[4] Greenwell, M. and Rahman, P. (2015) Medicinal Plants: Their Use in Anticancer Treatment. *International Journal of Pharmaceutical Sciences Research*, **6**, 4103-4112.

[5] Rahmani, A., Almatroudi, A., Alrumaihi, F. and Khan, A. (2018) Pharmacological and Therapeutic Potential of Neem (*Azadirachta indica*). *Pharmacognosy Reviews*, **12**, 250-255. https://doi.org/10.4103/phrev.phrev_8_18

[6] Sokei, J. (2018) Azadirachta Indica Bark Extract Stabilized Silver Nanoparticles: Antiproliferative Activity, Acute Toxicity Study and Antitumour Activity. Pan African University Institute for Basic Sciences Technology and Innovation (PAUSTI), Nairobi, Kenya.

[7] Siddiqui, I.A. and Sanna, V. (2016) Impact of Nanotechnology on the Delivery of Natural Products for Cancer Prevention and Therapy. *Molecular Nutrition & Food Research*, **60**, 1330-1341. https://doi.org/10.1002/mnfr.201600035

[8] Vazhappilly, C.G., *et al.* (2021) Current Methodologies to Refine Bioavailability, Delivery, and Therapeutic Efficacy of Plant Flavonoids in Cancer Treatment. *The Journal of Nutritional Biochemistry*, **94**, Article ID: 108623. https://doi.org/10.1016/j.jnutbio.2021.108623

[9] Pucci, C., Martinelli, C. and Ciofani, G. (2019) Innovative Approaches for Cancer Treatment: Current Perspectives and New Challenges. *Ecancermedicalscience*, **13**, Article No. 961. https://doi.org/10.3332/ecancer.2019.961

[10] Feng, B., Zhou, F., Wang, D., Xu, Z., Yu, H. and Li, Y. (2016) Gold Nanomaterials for Treatment of Metastatic Cancer. *Science China Chemistry*, **59**, 984-990. https://doi.org/10.1007/s11426-016-5593-0

[11] Şen, Ö., Emanet, M. and Ciofani, G. (2021) Nanotechnology-Based Strategies to Evaluate and Counteract Cancer Metastasis and Neoangiogenesis. *Advanced Healthcare Materials*, **10**, Article ID: 2002163. https://doi.org/10.1002/adhm.202002163

[12] Kargozar, S., Baino, F., Hamzehlou, S., Hamblin, M.R. and Mozafari, M. (2020) Nanotechnology for Angiogenesis: Opportunities and Challenges. *Chemical Society Reviews*, **49**, 5008-5057. https://doi.org/10.1039/C8CS01021H

[13] Jayson, G.C., Kerbel, R., Ellis, L.M. and Harris, A.L. (2016) Antiangiogenic Therapy in Oncology: Current Status and Future Directions. *The Lancet*, **388**, 518-529. https://doi.org/10.1016/S0140-6736(15)01088-0

[14] Singh, R.P. and Agarwal, R. (2007) Inducible Nitric Oxide Synthase-Vascular Endothelial Growth Factor Axis: A Potential Target to Inhibit Tumor Angiogenesis by Dietary Agents. *Current Cancer Drug Targets*, **7**, 475-483. https://doi.org/10.2174/156800907781386632

[15] Lala, P.K. and Orucevic, A. (1998) Role of Nitric Oxide in Tumor Progression: Lessons from Experimental Tumors. *Cancer and Metastasis Reviews*, **17**, 91-106. https://doi.org/10.1023/A:1005960822365

[16] Nematollahi, S., Nematbakhsh, M., Haghjooyjavanmard, S., Khazaei, M. and Salehi, M. (2009) Inducible Nitric Oxide Synthase Modulates Angiogenesis in Ischemic Hindlimb of Rat. *Biomedical Papers*, **153**, 125-129.

[17] Bielenberg, D.R. and Zetter, B.R. (2015) The Contribution of Angiogenesis to the Process of Metastasis. *The Cancer Journal*, **21**, 267-273. https://doi.org/10.1097/PPO.0000000000000138

[18] Gonciar, D., *et al.* (2019) Nanotechnology in Metastatic Cancer Treatment: Current Achievements and Future Research Trends. *Journal of Cancer*, **10**, 1358-1369.

https://doi.org/10.7150/jca.28394

[19] Gurunathan, S., Lee, K.J., Kalishwaralal, K., Sheikpranbabu, S., Vaidyanathan, R. and Eom, S.H. (2009) Antiangiogenic Properties of Silver Nanoparticles. *Biomaterials*, **30**, 6341-6350. https://doi.org/10.1016/j.biomaterials.2009.08.008

[20] Hareesh, K., Williams, J.F., Dhole, N.A., Kodam, K.M., Bhoraskar, V.N. and Dhole, S.D. (2016) Bio-Green Synthesis of Ag-GO, Au-GO and Ag-Au-GO Nanocomposites Using *Azadirachta indica*: Its Application in SERS and Cell Viability. *Materials Research Express*, **3**, Article ID: 75010. https://doi.org/10.1088/2053-1591/3/7/075010

[21] Ivanova, N., Gugleva, V., Dobreva, M., Pehlivanov, I., Stefanov, S. and Andonova, V. (2018) Silver Nanoparticles as Multi-Functional Drug Delivery Systems. In: Farrukh, M.A., Ed., *Nanomedicines*, IntechOpen, London, 71-91. https://doi.org/10.5772/intechopen.80238

[22] Kitimu, S.R., Kirira, P., Ochwangi, D., Mwitari, P. and Maina, N. (2022) Biogenic Synthesis of Silver Nanoparticles Using *Azadirachta indica* Methanolic Bark Extract and Their Anti-Proliferative Activities against DU-145 Human Prostate Cancer Cells. *African Journal of Biotechnology*, **21**, 64-72. https://doi.org/10.5897/AJB2021.17420

[23] Lokman, N.A., Elder, A.S.F., Ricciardelli, C. and Oehler, M.K. (2012) Chick Chorioallantoic Membrane (CAM) Assay as an *in Vivo* Model to Study the Effect of Newly Identified Molecules on Ovarian Cancer Invasion and Metastasis. *International Journal of Molecular Sciences*, **13**, 9959-9970. https://doi.org/10.3390/ijms13089959

[24] Baharara, J., Namvar, F., Mousavi, M., Ramezani, T. and Mohamad, R. (2014) Anti-Angiogenesis Effect of Biogenic Silver Nanoparticles Synthesized Using *Saliva officinalis* on Chick Chorioalantoic Membrane (CAM). *Molecules*, **19**, 13498-13508. https://doi.org/10.3390/molecules190913498

[25] Bokariya, P., Kothari, R., Gujar, V.K. and Shende, M.R. (2015) Teratogenic Effects of Insulin: An Experimental Study on Developing Chick Embryo. *Indian Journal of Pharmacology*, **47**, 212-214.

[26] Abdille, A.A., Kimani, J., Wamunyokoli, F., Bulimo, W., Gavamukulya, Y. and Maina, E.N. (2021) Dermaseptin B2's Anti-Proliferative Activity and down Regulation of Anti-Proliferative, Angiogenic and Metastatic Genes in Rhabdomyosarcoma RD Cells *in Vitro*. *Advances in Bioscience and Biotechnology*, **12**, 337-359. https://doi.org/10.4236/abb.2021.1210022

[27] Nirmali, W.K.R., Warnakula, L., Cooray, R., Hapuarachchi, N.S. and Magamage, M.P.S. (2019) Determination of Testicular Estrogen Receptor Alpha Expression of Male Chickens (*Gallus domesticus*) with Age. *Veterinary World*, **12**, 994-997. https://doi.org/10.14202/vetworld.2019.994-997

[28] Mahapatra, S., *et al.* (2011) Novel Molecular Targets of *Azadirachta indica* Associated with Inhibition of Tumor Growth in Prostate Cancer. *The AAPS Journal*, **13**, 365-377. https://doi.org/10.1208/s12248-011-9279-4

[29] Ribatti, D. (2017) The Chick Embryo Chorioallantoic Membrane (CAM) Assay. *Reproductive Toxicology*, **70**, 97-101. https://doi.org/10.1016/j.reprotox.2016.11.004

[30] Aydın, A., Sipahi, H. and Charehsaz, M. (2012) Nanoparticles Toxicity and Their Routes of Exposures. In: Sezer, A.D., Ed., *Recent Advances in Novel Drug Carrier Systems*, IntechOpen, London, 483-500. https://doi.org/10.5772/51230

[31] Hassanen, E.I., Morsy, E.A., Hussien, A.M., Ibrahim, M.A. and Farroh, K.Y. (2020)

The Effect of Different Concentrations of Gold Nanoparticles on Growth Performance, Toxicopathological and Immunological Parameters of Broiler Chickens. *Bioscience Reports*, **40**, BSR20194296. https://doi.org/10.1042/BSR20194296

[32] Kang, K., *et al.* (2011) Vascular Tube Formation and Angiogenesis Induced by Polyvinylpyrrolidone-Coated Silver Nanoparticles. *Toxicology Letters*, **205**, 227-234. https://doi.org/10.1016/j.toxlet.2011.05.1033

[33] Pradhan, R., Chatterjee, S., Hembram, K.C., Sethy, C., Mandal, M. and Kundu, C.N. (2021) Nano Formulated Resveratrol Inhibits Metastasis and Angiogenesis by Reducing Inflammatory Cytokines in Oral Cancer Cells by Targeting Tumor Associated Macrophages. *The Journal of Nutritional Biochemistry*, **92**, Article ID: 108624. https://doi.org/10.1016/j.jnutbio.2021.108624

[34] Lee, S.H., Jeong, D., Han, Y.S. and Baek, M.J. (2015) Pivotal Role of Vascular Endothelial Growth Factor Pathway in Tumor Angiogenesis. *Annals of Surgical Treatment and Research*, **89**, 1-8.

[35] Hajebi, S., Tabrizi, M.H., Moghaddam, M.N., Shahraki, F. and Yadamani, S. (2019) Rapeseed Flower Pollen Bio-Green Synthesized Silver Nanoparticles: A Promising Antioxidant, Anticancer and Antiangiogenic Compound. *JBIC Journal of Biological Inorganic Chemistry*, **24**, 395-404. https://doi.org/10.1007/s00775-019-01655-4

[36] Hood, J. and Granger, H.J. (1998) Protein Kinase G Mediates Vascular Endothelial Growth Factor-Induced Raf-1 Activation and Proliferation in Human Endothelial Cells. *Journal of Biological Chemistry*, **273**, 23504-23508. https://doi.org/10.1074/jbc.273.36.23504

[37] Zaitone, S.A. and Abo-Gresha, N.M. (2012) Rosuvastatin Promotes Angiogenesis and Reverses Isoproterenol-Induced Acute Myocardial Infarction in Rats: Role of iNOS and VEGF. *European Journal of Pharmacology*, **691**, 134-142. https://doi.org/10.1016/j.ejphar.2012.06.022

[38] Gavamukulya, Y., *et al.* (2021) *Annona muricata* Silver Nanoparticles Exhibit Strong Anticancer Activities against Cervical and Prostate Adenocarcinomas through Regulation of CASP9 and the CXCL1/CXCR2 Genes Axis. *Tumor Biology*, **43**, 37-55. https://doi.org/10.3233/TUB-200058

[39] Kramer, N., *et al.* (2013) *In Vitro* Cell Migration and Invasion Assays. *Mutation Research/Reviews in Mutation Research*, **752**, 10-24. https://doi.org/10.1016/j.mrrev.2012.08.001

[40] Gao, W., *et al.* (2018) Enhanced Diabetic Wound Healing by Electrospun Core-Sheath Fibers Loaded with Dimethyloxalylglycine. *Journal of Materials Chemistry B*, **6**, 277-288. https://doi.org/10.1039/C7TB02342A